

# **Sulfur Dioxide in the Venus Atmosphere: II. Spatial and temporal variability**

A.C. Vandaele<sup>a,†</sup>, O. Korablev<sup>b,c</sup>, D. Belyaev<sup>b</sup>, S. Chamberlain<sup>a</sup>, D. Evdokimova<sup>b</sup>, Th. Encrenaz<sup>d</sup>, L. Esposito<sup>e</sup>, K.L. Jessup<sup>f,g</sup>, F. Lefèvre<sup>h</sup>, S. Limaye<sup>i</sup>, A. Mahieux<sup>aj</sup>, E. Marcq<sup>k</sup>, F.P. Mills<sup>g,l</sup>, F. Montmessin<sup>k</sup>, C.D. Parkinson<sup>m</sup>, S. Robert<sup>a</sup>, T. Roman<sup>n</sup>, B. Sandor<sup>o</sup>, A. Stolzenbach<sup>h</sup>, C. Wilson<sup>p</sup>, V. Wilquet<sup>a</sup>

<sup>a</sup> Planetary Aeronomy, Royal Belgian Institute for Space Aeronomy, Brussels, Belgium

<sup>b</sup> Space Research Institute (IKI), Moscow 117997, Russia

<sup>c</sup> Moscow Institute of Physics and Technology (MIPT), Dolgoprudny 141700, Russia

<sup>d</sup> Observatoire Paris-Site de Meudon (LESIA), Meudon, France

<sup>e</sup> LASP - University of Colorado, Boulder, CO 80303-7814, USA

<sup>f</sup> Department of Space Science, Southwest Research Institute, Boulder, CO 80302, USA

<sup>g</sup> Fenner School of Environment and Society, Australian National University, ACT, Australia

<sup>h</sup> LATMOS, CNRS, Université Pierre et Marie Curie, Paris, France

<sup>i</sup> University of Wisconsin-Madison, Madison, WI 53706, USA

<sup>j</sup> Fonds National de la Recherche Scientifique, rue d'Égmond 5, 1000 Brussels, Belgium

<sup>k</sup> LATMOS, CNRS, Université de Versailles Saint-Quentin-en-Yvelines, Guyancourt, France

<sup>l</sup> Space Science Institute, Boulder, CO, 80303, USA

<sup>m</sup> University of Michigan, Ann Arbor, MI, 48109 USA

<sup>n</sup> Space Telescope Science Institute, Baltimore, MD 21218, USA

<sup>o</sup> University of Oxford, UK

<sup>†</sup> to whom correspondence should be sent ([a-c.vandaele@aeronomie.be](mailto:a-c.vandaele@aeronomie.be) - Planetary Aeronomy, Royal Belgian Institute for Space Aeronomy, Avenue Circulaire 3, 1180 Brussels, Belgium – Tel: +32(0)2-373.03.67)

## **Abstract**

The vertical distribution of sulfur species in the Venus atmosphere has been investigated and discussed in Part I of this series of papers dealing with the variability of SO<sub>2</sub> on Venus. In this second part, we have focused our attention on the spatial (horizontal) and temporal variability exhibited by SO<sub>2</sub>. Appropriate data sets – SPICAV/UV nadir observations from Venus Express, ground-based ALMA and TEXES, as well as UV observation on the Hubble Space Telescope – have been considered for this analysis. High variability both on short-term and short-scale are observed. The long-term trend observed by these instruments shows a succession of rapid increases followed by slow decreases in the SO<sub>2</sub> abundance at the cloud top level, implying that the transport of air from lower altitudes plays an important role. The origins of the larger amplitude short-scale, short-term variability observed at the cloud tops are not yet known but are likely also connected to variations in vertical transport of SO<sub>2</sub> and possibly to variations in the abundance and production and loss of H<sub>2</sub>O, H<sub>2</sub>SO<sub>4</sub>, and S<sub>x</sub>.

## **Keywords**

Atmospheric model; reference atmosphere; Venus; sulfur cycle

## 1 Introduction

The sulfur-oxide chemical cycle is a crucial component of the Venus atmosphere impacting its radiative balance in two key ways: (1) It determines the abundance of S, O, SO, SO<sub>2</sub>, and SO<sub>3</sub> in the atmosphere, all of which are needed for the formation of Venus' dense H<sub>2</sub>SO<sub>4</sub> cloud cover; (2) Some studies have suggested that the unknown UV absorber could be a sulfur-bearing compound and could be responsible for up to 50% of the energy deposited in Venus' mesosphere [1-3]. The recent Frandsen et al. [2] paper gives quite strong evidence of the existence of a S-based UV absorber (namely, a mixture of cis- and trans-OSSO). Lee et al. [3] exhibited an anti-correlation between UV absorber and SO<sub>2</sub> content in the data sets of VMC and SPICAV-UV on board Venus Express, easily explained if there is some conversion between both species. Additionally, to date, no theoretical model (photochemical or dynamical) has been able to replicate the observed H<sub>2</sub>SO<sub>4</sub> formation rate in a way that is also consistent with the observed abundances of other Venus atmosphere gases (see [4] and references therein). Indeed at the cloud top region, all photochemical models encounter problems because the oxidation state in these models differs from what can be inferred from observations of oxygen upper limits. In the upper mesosphere, models cannot explain the SO<sub>2</sub> inversion layer if they use H<sub>2</sub>SO<sub>4</sub> as the source of the upper mesospheric SO<sub>2</sub>.

SO<sub>2</sub> was detected in the Venus atmosphere, above, within and below the clouds, very early in the history of Venus exploration. The observations carried out by the Ultraviolet Spectrometer (UVS) on board *Pioneer Venus Orbiter* (PVO) [5] showed a steady decline of the UV cloud top (~ 40 mbar, 68 km) SO<sub>2</sub> content from 100 ppb down to 10 ppb about 10 years later [6]. The decline of the SO<sub>2</sub> amount was rather fast over the first year, and much slower later on (Figure 1). This behaviour was initially interpreted as evidence of a massive "injection of SO<sub>2</sub> into the Venus middle atmosphere by a volcanic explosion" [6]. This steep decline of the SO<sub>2</sub> abundance was also confirmed by IUE observations, which showed a decrease of the abundance from 380±70 ppb in 1979 down to 50±20 ppb in 1988 [7]. [8, 9]. In 1995 a first measurement from the Hubble Space Telescope was performed and yielded a value of 20±10 ppb [10] again confirming a decrease in the SO<sub>2</sub> abundance with time. All these observations concurred with the general vision that SO<sub>2</sub> abundance decreased from the 1970's to the 1990's. However, observations performed by SPICAV-UV show that the high levels of SO<sub>2</sub> were again observed in 2007-2008 [11, 12] followed again by a steep decrease, as shown in Figure 1.

The recent European *Venus Express* (VEx) mission marked a renewal in the interest of Venus. The VEx mission covered the 2006-2014 time period during which several other instruments on Earth and different platforms, such as the Hubble Space Telescope observed the planet's atmosphere. Combining different observations allows a more global view on the SO<sub>2</sub> distribution in the atmosphere. This paper is the second part in a series of articles investigating the variability of the sulfur species within the Venus atmosphere, with the focus set on the spatial (horizontal) and temporal variability. Several data sets – SPICAV/UV nadir observations from *Venus Express*, ground-based ALMA and TEXES, as well as STIS UV

observation on the Hubble Space Telescope – have been considered for this analysis. We will investigate different aspects of the variability of the sulfur, i.e. short and long-term, short-scale.

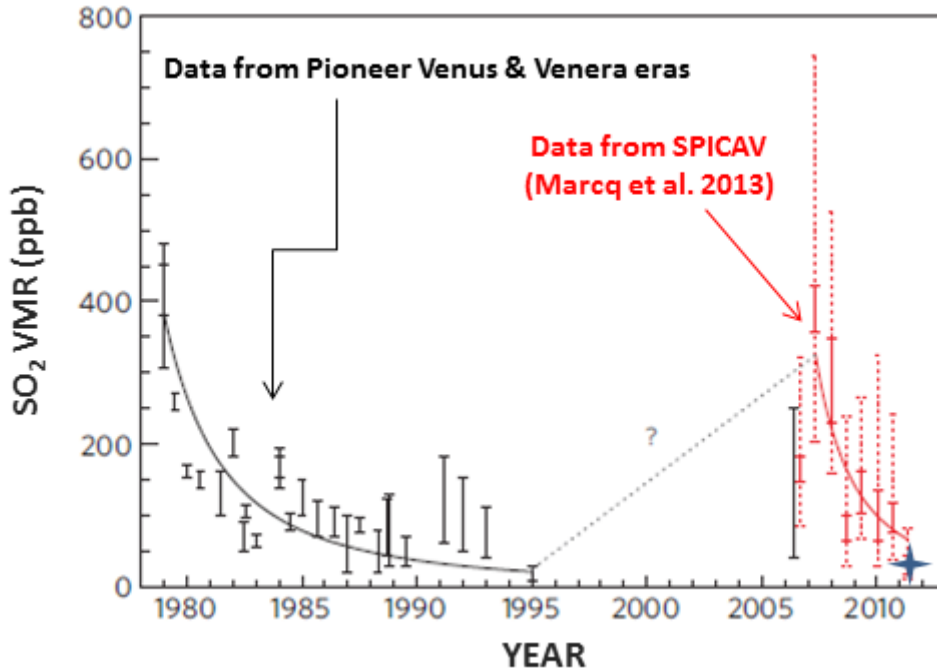


Figure 1: More than thirty years of  $\text{SO}_2$  measurements at Venus’s UV cloud top ( $\sim 60\text{-}80$  km). Black: previous measurements retrieved from Earth-based and Venus orbiting platforms (see Table I) [13]. Red: 8-month moving average of SPICAV data. Error bars are  $1\sigma$  random uncertainty, and dotted red error bars represent measurement dispersion in each temporal bin. Blue cross: average of the 2010+2011 HST dayside observations. Figure from [14].

## 2 Observations

In Part I of this series of paper, we described instruments and data sets from which information can be derived on the vertical distribution of SO and  $\text{SO}_2$  within the Venus atmosphere. This encompassed solar and stellar observations performed by the SPICAV/UV and SPICAV/SOIR instruments on board *Venus Express*, as well as the sub-mm ground-based observations from the JCMT.

In this second Part of the series, we will focus on instruments and techniques that provide knowledge on the spatial, here horizontal, distribution. The following instruments and observations have been considered: nadir observations with SPICAV/UV (on board VEx), STIS observations on the Hubble space Telescope (HST), and ground-based observations (ALMA, TEXES).

## 2.1 SPICAV/UV – nadir observations

The SPICAV instrument on board VEx was a spectrometer very similar to SPICAM, part of the payload of the Mars Express orbiter [15, 16]. Its UV channel operated in the 118-320 nm spectral range with a resolution of 1.5 nm at nadir or stellar/solar occultation modes. This instrument has already been described in Part I of this series of papers, only details concerning the nadir observations will be given here.

SO<sub>2</sub> UV absorption near 220 nm and 280 nm can also be measured by the UV channel of the SPICAV instrument on board VEx [16] in nadir mode, thanks to the scattering of solar UV light at cloud top level (~75 km) [11, 12]. The processed data set consists of UV spectra at a moderate spectral resolution ( $R \sim 200$ ) acquired during 299 orbits. About 45 % of these orbits were acquired in near nadir pointing (emission angle smaller than 1°), sweeping large latitudinal swaths with an emphasis on the northern hemisphere due to VEx orbital constraints. The remainder have been acquired in other near nadir pointing science modes, with emission angles rarely exceeding 30°. More recently, starting in September 2013, a new science mode was set up initially for mapping NO and O<sub>2</sub> night glows. This mode adds a lateral “wobbling” to the pointing, which, when combined with the usual latitudinal orbital sweeping, yields a lacunar 2D mapping ability. Only a handful of these newer observations have been examined thus far. These new data were processed with an updated version of the radiative transfer model designed to more adequately handle the spectrally resolved HST observations [14]. In due course, the whole SPICAV-UV data set will be reprocessed using consistently the same model.

Observations were usually averaged by several tens of spectra, in order to increase the signal to noise ratio, as well as speeding up further processing. These spectra are then calibrated in wavelength and spectral radiance, and finally converted into spectral reflectance through division by a standard SOLSPEC solar spectrum [17]. The exact procedure is described extensively in [11]. A forward radiative transfer model is then run through a Levenberg-Marquardt fitting algorithm in order to derive local SO<sub>2</sub> column densities above the cloud top (defined as the unity optical depth altitude level at 250 nm, ~ 75 km with the assumed aerosol extinction profile). Inversion of these column densities into local mixing ratios depends on a prescribed vertical profile for both cloud opacity and SO<sub>2</sub>. The exact vertical profiles cannot be directly retrieved from these observations but have to be assumed to be based on vertically resolved measurements and/or models such as Belyaev et al. [18, 19]. A scale height of 3 km for both SO and SO<sub>2</sub> was therefore assumed, with both species increasing with decreasing altitude down to the level where SO<sub>2</sub> mixing ratio reaches 150 ppmv. Also, since SPICAV-UV cannot resolve their individual spectral lines, SO could not be retrieved independently from SO<sub>2</sub> and was assumed to be tied to 10% of the local mixing ratio of SO<sub>2</sub>. Moreover, the actual cloud extinction vertical profiles exhibit large spatial and temporal variations (whereas the radiative transfer model assumes a static cloud and haze background detailed in [11, 12]), so that the conversion factor between column densities above the unity optical depth and abundances at a reference altitude is not constant and may also vary by a factor of about 2

[11] around a typical value of 1  $\mu\text{m-atm}$  for 10 ppb at 72 km. The details of the fitting procedure and radiative transfer model are extensively described in [11, 12]. Also, a sensitivity study reported in [12] (suppl. Material) shows that column densities of  $\text{SO}_2$  lower than 10  $\mu\text{m-atm}$  are not as robustly retrieved as those above this threshold due to partial degeneracy with the unknown UV absorber signature, and should be merely viewed as being bracketed in the 1 to 10  $\mu\text{m-atm}$  range.

**2.2 Hubble Space Telescope**

UV spectra of Venus were obtained using the Hubble Space Telescope / STIS instrument on December 28, 2010; January 22, 2011; and, January 27, 2011 [14]. The HST/STIS data was acquired using the G230LB (170-317 nm) grating, with the 52"x0.1" slit and the CCD detector (0.51" pixels), to obtain high spectral (0.27 nm) and spatial (40-60 km/pixel, assuming 2 pixel binning) resolution measurements of Venus'  $\text{SO}_2$  and SO gas absorption signatures (Figure 2). On each date, the 52" HST/STIS slit was centred on the morning terminator longitude, so that Venus' morning quadrant was observed from the terminator to the sunlit limb. On each date Venus was observed with the HST/STIS slit in its nominal pointing position, i.e. the slit was oriented at a 45° angle relative to Venus' equator. In this orientation, a different time of day and latitude was recorded in each pixel. In order to build up a picture of the  $\text{SO}_2$  and SO gas absorption signatures as a function of time of day at multiple latitudes, two exposures were taken on each visit, and in each exposure the centre of the 52" slit intersects the morning terminator longitude at a single unique latitude (Figure 2, Table 1).

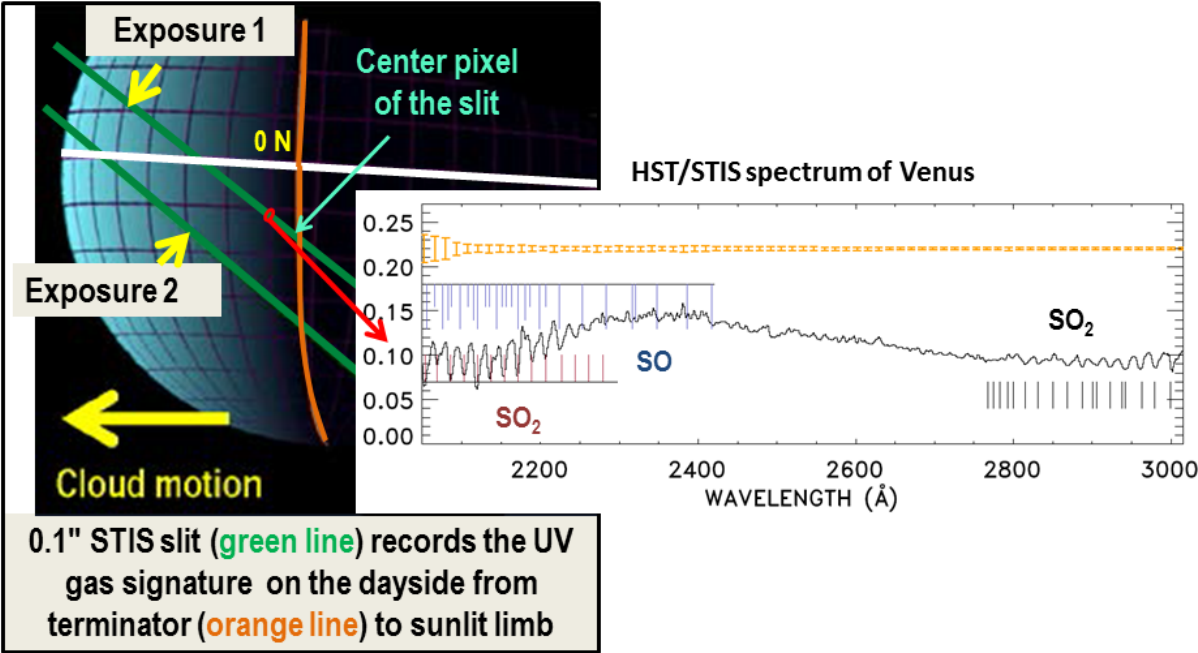


Figure 2: On the left, a representative schematic of the HST/STIS slit orientation is provided. Two exposures were taken on each date and in each exposure the centre of the HST/STIS slit (green lines) intersects the morning terminator longitude (orange line) at a single latitude. On the right a representative HST/STIS spectrum of Venus' reflectivity is plotted showing the position of the SO<sub>2</sub> and SO gas absorption signatures. The band heads for the SO<sub>2</sub> B-X transitions (180-240 nm), SO<sub>2</sub> A-X transitions (280-310 nm), and SO B-X transitions (190-240 nm) are as indicated by the red, black and blue lines, respectively. The uncertainty in the data is indicated by the orange error bars.

Table 1: Observational Conditions for the 170-320 nm HST/STIS Observations taken during the *Venus Express* Era

OBS NUMBER	date (yyyy-mm-dd)	target <sup>1</sup> latitude	terminator longitude	sub-earth longitude	Planet radius (arcsec)	% illuminated	mid-exposure time (UT)	exposure length (s)
0	2010-12-28	15 S	65E	72.4 E	14.3	44%	00:21:54	153
1	2010-12-28	32 S	65E	72.5 E	14.3	44%	01:58:21	153
2	2011-01-22	45 S	145E	136.6 E	10.7	57%	17:03:55	58
3	2011-01-22	65 S	145E	136.8 E	10.7	57%	18:39:38	58
4	2011-01-27	45 S	160E	149.4 E	10.2	59%	15:20:20	116
5	2011-01-27	65 S	160E	149.5 E	10.2	59%	16:56:13	116

1: The latitude at which the HST/STIS slit crossed the morning terminator.

The HST/STIS instrument was the only instrument able to obtain instantaneous and simultaneous mapping of the SO<sub>2</sub> and SO gas local time variation from the AM terminator towards local noon (recording reflected sunlight data at solar zenith angles (SZA) ~ 15-80°) during the lifetime of the Venus Express Mission. Taking advantage of this unique capability, the HST/STIS observations were taken in coordination with a number of observing campaigns, including ground based sub-mm observations [14], solar occultation observations made at the dawn terminator by VEx/SOIR on December 28, 2010 [14] and cloud top monitoring images obtained by VEx/VMC and VEx/VIRTIS obtained in January, 2011. Ground based sub-mm observations of Venus' upper mesosphere were obtained contemporaneously with the HST on all dates - allowing direct comparison of the upper mesospheric SO<sub>x</sub> abundances and the upper cloud deck SO<sub>x</sub> abundances. On December 28, 2010, the HST observations were obtained with the slit crossing the terminator at the tangent latitude above which SOIR was simultaneously obtaining occultation measurements. This coordinated effort provided the first opportunity to acquire measurements of Venus' dayside

cloud top local time SO<sub>2</sub> variability over a time period extending from within ±30 minutes from dawn (i.e., for SZA ~ 90±8°) - via SOIR, to near local noon, without any temporal disparity between the two measurements. These measurements have provided the first unambiguous empirical data from which the photochemical processing of Venus' SO<sub>x</sub> species has been modelled and investigated. Similarly, the simultaneous acquisition of HST spectral data and VEx/VMC and VIRTIS imaging provided a means to directly investigate the impact of the local and latitudinal changes in the cloud top SO<sub>x</sub> abundance to the observed cloud top brightness.

### 2.3 *TEXES*

TEXES (Texas Echelon-Cross-Echelle Spectrograph) is an infrared imaging spectrometer operating between 5 and 25 μm, which has the advantage of combining high spectral (up to R = 80000) and spatial (about 1 arcsec) resolution. The instrument was developed by J. H. Lacy from the University of Texas [20] and is now operated by M. J. Richter (University of California Davis, CA) and T. K. Greathouse (SwRI, San Antonio, TX). Since 2001, TEXES has been used as a visitor instrument on the NASA Infrared Telescope Facility (IRTF) at Mauna Kea Observatory. In the case of planetary atmospheres, the instrument allows the observer to select several transitions of a set of atmospheric species, by selecting an appropriate spectral range (covering typically 5 to 10 cm<sup>-1</sup>), and to monitor their abundances over the planetary disk. It is thus well designed for studying day/night or morning/evening variations, as global maps are obtained in a single observation.

TEXES has been used to identify hydrogen peroxide (H<sub>2</sub>O<sub>2</sub>) on Mars [21] and to monitor the abundances of H<sub>2</sub>O<sub>2</sub> and H<sub>2</sub>O (through its proxy HDO) as a function of the seasonal cycle [22]. The method consists in the simultaneous observation of weak individual lines of the minor species that are compared to weak transitions of the main atmospheric constituent CO<sub>2</sub>. This method provides an estimate of the mixing ratio of the minor species, as well as its evolution in space and time. Since 2012, this method has been applied on Venus to monitor simultaneously the variations of sulfur dioxide SO<sub>2</sub> and HDO within the 60-85 km altitude range as a function of time and space [23, 24]. The main result of this study is evidence for fast variations of SO<sub>2</sub> in space and time (within a timescale of a few hours) while, in contrast, the water vapour distribution remains more or less constant over the disk and over time [25]. Analysis of the available TEXES data indicates that there is a cut-off in the SO<sub>2</sub> abundance at ~ 67 km, such that the SO<sub>2</sub> abundance above this cut-off is lower than that observed below and its magnitude cannot exceed a few ppb (from 2-4 ppb [24] to 10 ppb).

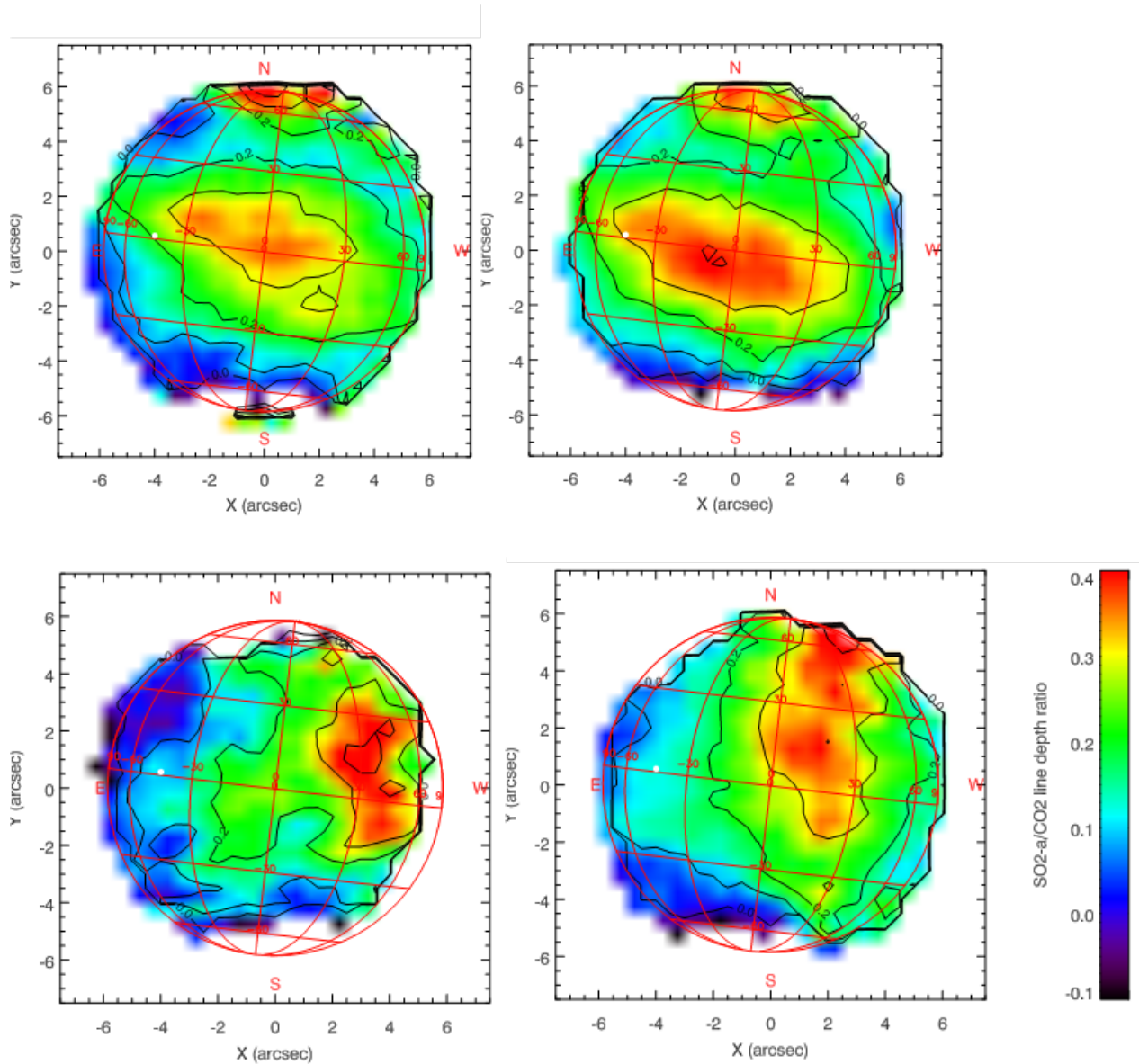


Figure 3: Variations of the  $\text{SO}_2/\text{CO}_2$  line depth ratio in July 2014 as measured by TEXES. From left to right: July 7, 17:00 UT; July 7, 20:00 UT; July 8, 17:00 UT, July 8, 20:00 UT. The  $\text{SO}_2$  transition is at  $1345.12 \text{ cm}^{-1}$ , the  $\text{CO}_2$  transition is at  $1345.25 \text{ cm}^{-1}$ . The disk-integrated  $\text{SO}_2$  mixing ratio at the cloud top is about 100 ppb. The morning terminator is observed on the right side of the disk. The subsolar point is indicated with a black cross. The  $\text{SO}_2$  volume mixing ratio (vmr) can be derived from the line depth ratio (ldr) using a linear relation, as shown in Encrenaz et al. [26]  $\text{vmr}(\text{SO}_2)(\text{ppbv}) = \text{ldr}(\text{SO}_2/\text{CO}_2) \times 600$ . The full scale ( $\text{ldr} = 0.4$  corresponds to a  $\text{SO}_2$  mixing ratio of 240 ppbv.

## 2.4 ALMA

ALMA (Atacama Large Millimeter/Submillimeter Array) is a network of 66 antennas, with diameters ranging from 7 to 12 meters and separations ranging from 150 m to 16 km, operating in the interferometric mode in the millimetre and submillimetre ranges. The array is located in the Atacama desert (Chile) at an altitude of 5100 m. Observations of Venus were

obtained in the Early Phase (Cycle 0) in November 2011, with 16 antennas of 12 m in diameter, in compact configuration. The diameter of Venus was 11 arcsec and the spatial resolution was about 2 arcsec.

Transitions of CO, SO, SO<sub>2</sub> and HDO were simultaneously recorded around 345 GHz during four sequences of 30 minutes each, on November 14, 15, 26 and 27, 2011. The submillimetre range probes the upper atmosphere of Venus, at altitudes ranging from about 70 km to 110 km. Maps of SO, SO<sub>2</sub> and HDO have been retrieved from the Nov. 14 and Nov. 15 data. Significant variations appear across the disk and within a timescale of one day. Like the sub-mm JCMT data, the retrieval of the SO<sub>2</sub> and SO mixing ratios are dependent on the assumed vertical profile shape for SO<sub>2</sub> and SO. On Nov. 14, the SO and SO<sub>2</sub> vertical distributions exhibited a cut-off at about 88 km. If the vertical profile below the cut-off altitude is linear, then there are no sulfur species below the cut-off altitude and mixing ratios of about 8 ppb (SO) and 12 ppb (SO<sub>2</sub>) are seen above this level. The HDO spectrum is consistent with a water vapour mixing ratio of about 2.5 ppm, constant with altitude [27].

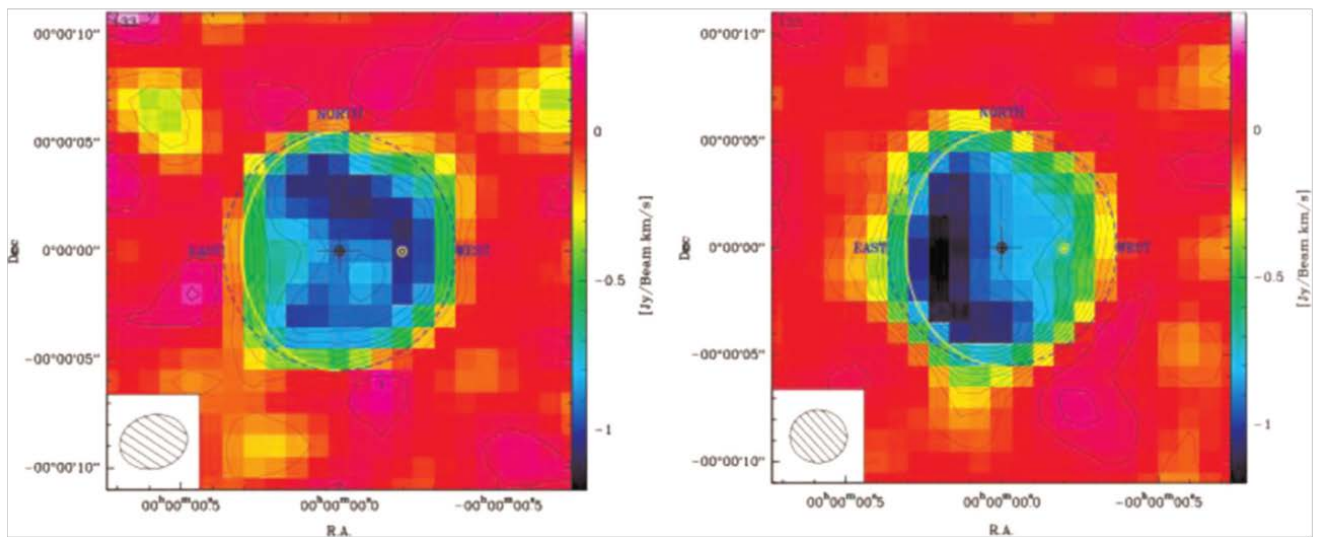


Figure 4: ALMA maps of the intensities of the SO transition (top) and the SO<sub>2</sub> transition (bottom) on Venus at 346.528 GHz (SO) and 346.652 GHz (SO<sub>2</sub>) on November 14 (left) and November 15 (right). The diameter of the planet is 11 arcsec. The maps are inferred from the line equivalent widths. The unit is Jy/beam.km/s. The synthesised beam is 3.23 x 2.50 arcsec on Nov. 14 and 2.74 x 2.48 arcsec on Nov. 15. The beam size is shown in the lower left corner of each figure. The central dashed black circle represents the diameter of the planet. The yellow dashed curve represents the evening terminator. The maximum scale corresponds to a line equivalent beam of -1.2 Jy/beam/km.s for the SO maps and -1 Jy/beam/km.s for the SO<sub>2</sub> maps. The SO<sub>2</sub> maps show a distinct decrease of the SO<sub>2</sub> abundance between Nov. 14 and Nov. 15, 2011.

### 3 Analysis and discussion

The different data sets described above and in Part I of this series of papers, have been analysed in order to derive information on the SO<sub>2</sub> variability within the Venus atmosphere in terms of spatial and temporal variations, on different scales (short/long).

#### 3.1 Short scale and short-term variations

Spectroscopic imaging of the Venus disk, as observed from the ground or from Earth orbit, allows us to track short-scale and short-term variations of the Venus atmosphere. Here short-term means on a timescale smaller than the atmospheric rotation rate. This information is fully complementary to the *Venus Express* observations. Indeed, in-orbit observations are often associated with a constant local time and cannot easily cover a whole range of latitudes, longitudes and local times instantaneously. However, we will show that the so-called “sweeping mode” implemented for some late SPICAV/UV nadir observations enables some mapping ability of the dayside 70-80 km SO<sub>2</sub> distribution.

##### 3.1.1 Short-scale variations

Full disk spatially resolved SO<sub>2</sub> mapping on Venus has been obtained, in particular, by two facilities: TEXES at the IRTF telescope in the thermal infrared (7 and 19  $\mu\text{m}$ ) and ALMA in the submillimetre range. Infrared observations probe the lower mesosphere, above the cloud

top (60-85 km at 7  $\mu\text{m}$ ) or a few km below (from within the clouds to about 85 km at 19  $\mu\text{m}$ ). In contrast, submillimetre observations probe the upper mesosphere above an altitude of 80 km. TEXES observations have been performed in January and October 2012, and later in February and July 2014 [23-25]. The integration time of each TEXES map is about 15 minutes. Four sessions of ALMA observations, each with a 30-minute integration time, have been performed on November 2011 [27].

Both TEXES and ALMA have the potential to see the day and night side  $\text{SO}_2$  abundance. TEXES observations have shown evidence for short-scale variations of  $\text{SO}_2$  over the observed Venus disk with local time. As shown in Figure 3, the  $\text{SO}_2$  variations at  $\sim 60$ -67 km (67 km being the cut-off altitude, above which no  $\text{SO}_2$  is seen by the TEXES instrument) show a contrast of about a factor of 5 across the disk (in the 7  $\mu\text{m}$  data). At  $\sim 57$ -67 km, a contrast of about a factor of 3 has been inferred from the 19  $\mu\text{m}$  data [24, 25]. Sub-mm observations obtained with ALMA, with the beam centred primarily above the dayside atmosphere, show that the contrast in the upper mesosphere, which is limited by the poor signal to noise, is at least a factor of 3 [27]. The  $\text{SO}_2$  distribution observed over the disk at  $\sim 60$ -67 km (at 7  $\mu\text{m}$ ) is patchy (Figure 3), with a local scale of about 800 km, corresponding to the spatial resolution of the instrument (1 arcsec over a 15- arcsec diameter, [25]). The  $\text{SO}_2$  distribution appears less patchy at  $\sim 57$ -67 km, with a local scale larger than the 3-arcsec spatial resolution [24]. TEXES observations displayed in Figure 3 show that while strong patterns can be seen in the dayside  $\text{SO}_2$  at the cloud-top, these patterns are transient in nature. For example, on July 7, the density at the equator appears to be enhanced relative to that observed at higher latitudes, at all local times extending from the sub-solar point to the terminator. However, a different pattern is observed on July 8: the equatorial absorption depth at the AM terminator is more enhanced than at the sub-solar point and the observed terminator enhancement is observed at most latitudes.

Only a few orbits from the SPICAV/UV nadir “sweeping mode” dataset have been analysed so far. They were acquired in late September 2013, when  $\text{SO}_2$  levels were quite low in average by Venus' standard. Nevertheless even during these observations the  $\text{SO}_2$  spatial distribution was strongly variable, such that the magnitude and location of the maximum  $\text{SO}_2$  column density detections varied between orbits. For example, during orbit #2710 (see Figure 5) in a localized “spot” no larger than a few degrees in latitude located near 22 S latitude the retrieved  $\text{SO}_2$  column density was 2 to 3 times higher than was observed at nearby latitudes. This is fully consistent with the patchy  $\text{SO}_2$  spatial distribution derived from TEXES and ALMA observations, as well as with their typical fluctuation scale length of a few hundred kilometers.

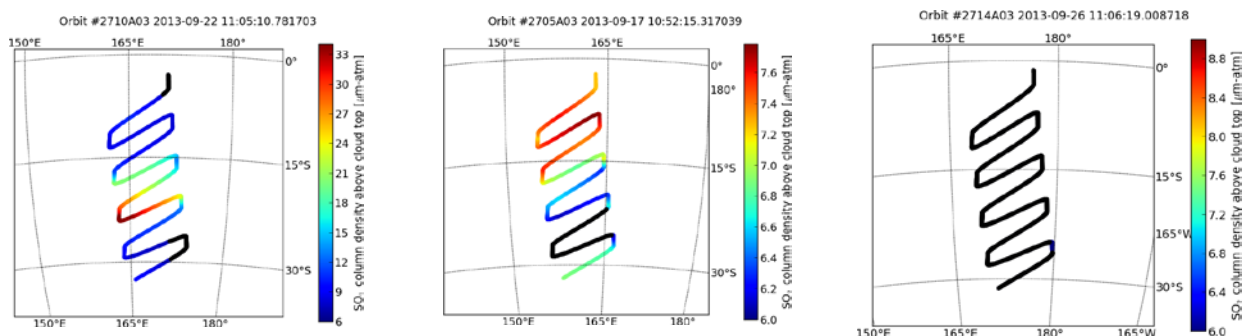


Figure 5: SPICAV/UV maps of  $\text{SO}_2$  column densities obtained in late September 2013, exhibiting significant short-scale spatial and temporal variability.

### 3.1.2 Variations with local time

Figure 6 shows the  $\text{SO}_2$  VMR values obtained by the different instruments as a function of the local solar time (LST), the instruments being represented by symbols, while the colour indicates the latitude at which the measurements have been performed. A clear enhancement of the abundance at and near both sides of the terminator and a minimum in  $\text{SO}_2$  near local solar noon are observed for the 70-80 km altitude range shown in the figure. It is hard to comment about local time variations in the other altitude ranges due to the lack of measurements in these regions. Similarly, in Figure 8, comparison of the early afternoon and terminator  $\text{SO}_2$  abundances retrieved between 70 and 80 km at  $\sim 60^\circ \text{N}$  latitude from SPICAV/UV and SOIR, respectively, suggests that at this latitude the terminator abundance is inflated above the mid-day  $\text{SO}_2$  abundance.

Note that the JCMT observations providing information above 80 km have been obtained at low latitudes (cyan dots) at which no occultation observations have been performed. This, and the very different spatial resolution of JCMT observations, render the direct comparison between the data sets shown in Figure 6 top two panels very difficult if not meaningless. Moreover, the current JCMT retrieval methods do not attempt to determine if increases in altitude inferred from SPICAV/SOIR occultation measurements over a limited spatial region agree or disagree with their inferred  $\text{SO}_2$  vertical distribution or abundance levels at altitudes above 80 km.

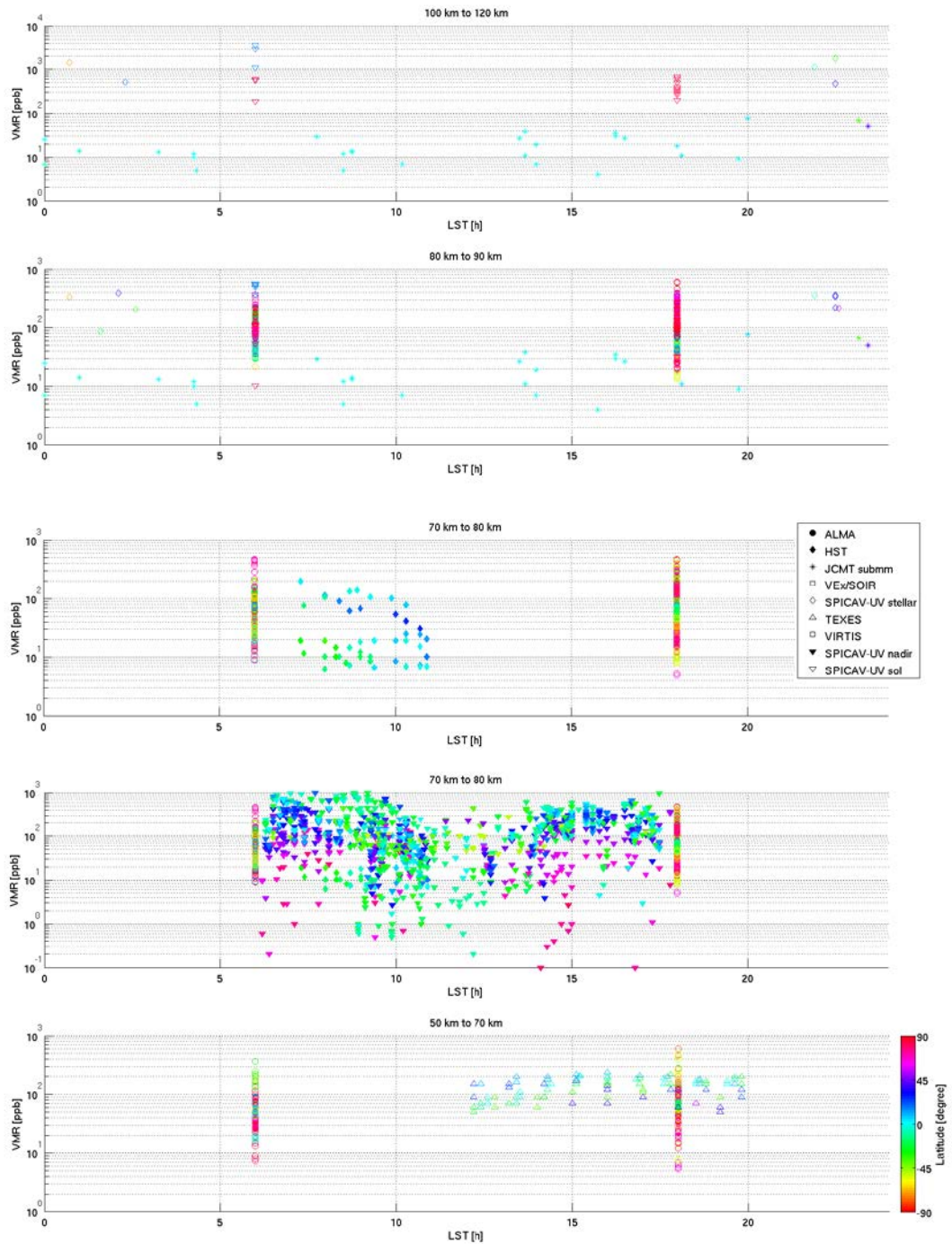


Figure 6:  $\text{SO}_2$  VMR as a function of local solar time (LST) for different altitude regions, from top to bottom: 100 to 120 km, 80 to 90 km, 70 to 80 km (all instruments except SPICAV-UV nadir), 70 to 80 km (all instruments), and 50 to 70 km. The colour code is the latitude.

The 2010 and 2011 HST/STIS observations [14] also show that the near AM terminator (i.e.,  $\text{SZA} \sim 60\text{-}75^\circ$ ) cloud top  $\text{SO}_2$  column density observed within a single latitude could be

nearly two times higher than that observed at the same latitude but at later local times (i.e. at smaller SZAs). However, as was true with the TEXES observations, the near-terminator enhancements appeared to be transient in nature. Additionally the HST results suggest that the existence of the near-AM terminator enhancements may in fact be dependent on the overall gas density present at the cloud top between 70 and 80 km.

Identical SO<sub>2</sub> densities were retrieved at ~ 70 and 100° SZA from the coordinated HST/STIS and VEx/SOIR observations obtained on December 28, 2010, between ~77±3 km near Venus' dawn terminator, i.e., within the 2 hour period extending from pre-dawn (5:30 AM local Venus time) to early-morning (7:30 AM local Venus time). Theoretical analysis of the relative balance between SO<sub>2</sub> photolysis and vertical and horizontal transport at low latitudes in Venus' middle atmosphere as a function of local time indicates that at 60-80 km and SZA > 50°, the atmosphere is not in photochemical equilibrium and dynamic transport dominates [14]. This implies that the pre-dawn SO<sub>2</sub> detected near 30S in the joint HST/STIS and SOIR observations was transported horizontally across the terminator with no significant modification to its abundance within a 2 hour period due to photochemical processing.

Photochemical models show that a SO<sub>2</sub> enhancement is expected at low latitudes at the terminator in the 65-100 km altitude range [14]. In the altitude range where the atmosphere is not in photochemical equilibrium (below 80 km), the exact magnitude of the near terminator SO<sub>2</sub> density is difficult to predict from 1-d photochemical models. Nevertheless, these models indicate that the SO<sub>2</sub> abundance at the terminator should be enhanced compared to values at later local times. Thus, photochemical modelling can reproduce the SO<sub>2</sub> enhancements sometimes observed at the terminator between 60 and 80 km altitude by TEXES and HST. However, the models that rely solely on the photochemical time scales do not provide an explanation for why enhancements in the SO<sub>2</sub> abundance at the terminator relative to later local times would be transiently observed.

Thus far, ALMA observations have probed the day side of the planet, and marginally the evening terminator at the limb. Above 80 km, the level of local scale SO<sub>2</sub> variability inferred from these data is similar to that inferred from the TEXES observations. Additionally, the November 2011 ALMA observations [27] also indicate that the level of local scale upper mesospheric SO variability is high and that enhancements of the SO gas can be seen on both near and far from the terminators (see Figure 4).

### 3.1.3 Short-term variations

Characterization of short-term variations in the SO<sub>x</sub> gas distributions can be performed using most of the instruments considered in this study. In Figure 7, which illustrates the time variations observed in SO<sub>2</sub> for the latitude region -20° to 20° over the lifetime of the VEx mission, the short-term (~24 hours) fluctuations SO<sub>2</sub> abundance clearly appear. Figure 7 and Figure 9 show that, over short periods of time (a few Earth days) the SO<sub>2</sub> abundance can vary over several orders of magnitude. Likewise Figure 9 shows that broad variations (~ 1-2 orders of magnitude) in the SO<sub>2</sub> abundance are observed at each latitude independent of the altitude

or observing platform. Since the SPICAV-UV nadir observations measure the column abundance of  $\text{SO}_2$  above the clouds it is reasonable to assume that some of the variation in the  $\text{SO}_2$  observations may be due to cloud-top altitude variations [11]. However, the cloud top altitude measured [28] during the *Venus Express* mission was found to be quite uniform and stable with time across the whole planet except towards the polar region. Thus, cloud top altitude variations are not likely to be the primary source of the observed  $\text{SO}_2$  column variability inferred from the SPICAV-UV nadir observations. More significantly, the SPICAV-UV nadir retrievals of  $\text{SO}_2$  abundances below roughly 100 ppb can actually lie within 10-100 ppb due to degeneracy in the retrieval with UV absorber abundances [12]. This effect may exaggerate to a degree the apparent range of  $\text{SO}_2$  variability. On the other hand, measurements like TEXES and solar/stellar occultations measure the ratio of  $\text{SO}_2$  to  $\text{CO}_2$ , giving a true mixing ratio unaffected by cloud-top altitude variations. These datasets also show variations in mesospheric  $\text{SO}_2$  abundances that are larger than an order of magnitude validating that variation in the  $\text{SO}_2$  abundances on the order of 1-2 orders of magnitude are observed for all latitudes (indicated by colour code) at all altitude ranges presented in Figure 9.

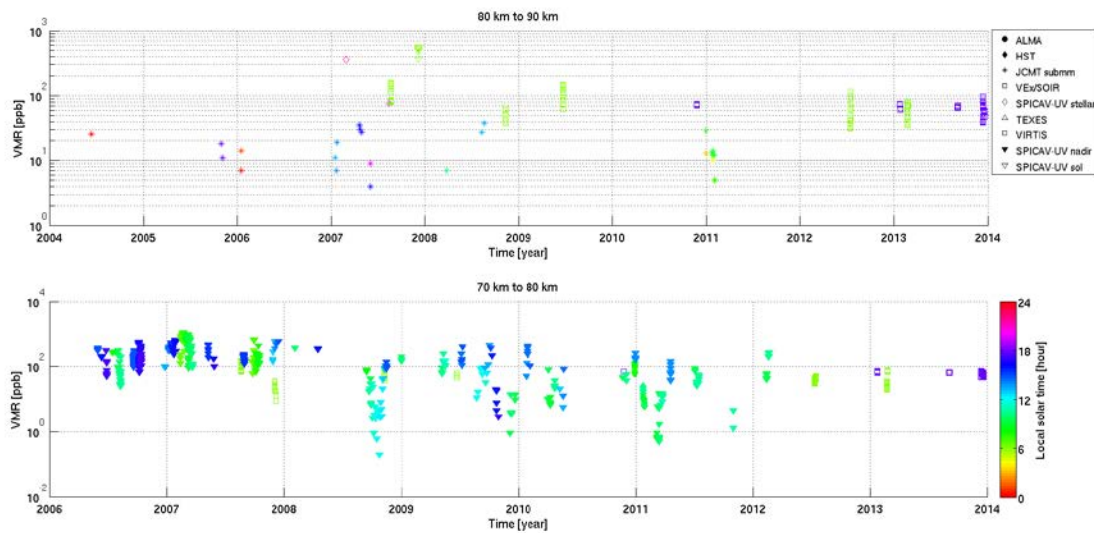


Figure 7: Variation of the  $\text{SO}_2$  VMR in two altitude regions (70 to 80 km and 80 to 90 km) as a function of the time for the latitude region  $-20^\circ$  to  $20^\circ$ . The colour code is the local solar time. The symbols represent the different instruments.

During TEXES observations, sequences have been repeated for the same local times and the same location on the disk, with a time scale ranging between a day (January 2012) and a couple of hours (October 2012, July 2014). Significant changes were observed in both cases near 60 km [24, 25]. Similarly, the SPICAV/UV nadir dataset records significant variability in the  $\text{SO}_2$  abundance and distribution within a few orbits (i.e., within a few Earth days). In these cases, fractional variability in the  $\text{SO}_2$  abundance tends to be larger during epochs where the  $\text{SO}_2$  abundance is high. For example, order of magnitude drops in the 70-80 km cloud top  $\text{SO}_2$  levels to values below the SPICAV/UV nadir detection threshold have occurred within just

four VEx orbits (Figure 4). Short-term variations within the clouds remain to be confirmed [25].

The reduction and analysis of the ALMA dataset is still in progress. Preliminary analysis of the ALMA data obtained on November 14 and 15, 2011 shows that the spatial SO<sub>2</sub> and SO distributions above 80 km change significantly over a timescale of one day [27]. In the case of SO<sub>2</sub>, there seems to be a significant decrease of the disk-integrated abundance from one day to the next, in agreement with the daily to weekly, variability suggested by JCMT hemispheric-scale observations [29]. In the case of SO, the disk-averaged abundance from ALMA observations appears more or less constant, but the maximum SO abundance shifts from the northern hemisphere in the morning to the southern hemisphere in the evening (Figure 4). JCMT observations, in contrast, suggest significant hemispheric-scale variability of SO abundance can occur on daily to weekly timescales [29]. It can be noticed that water vapour, observed with ALMA through its proxy HDO, also shows spatial and temporal variations in the upper mesosphere [27], while such variations are not observed with TEXES at ~60-67 km (at 7  $\mu$ m) or at ~57-67 km (at 19  $\mu$ m) (Figure 3) [24, 25].

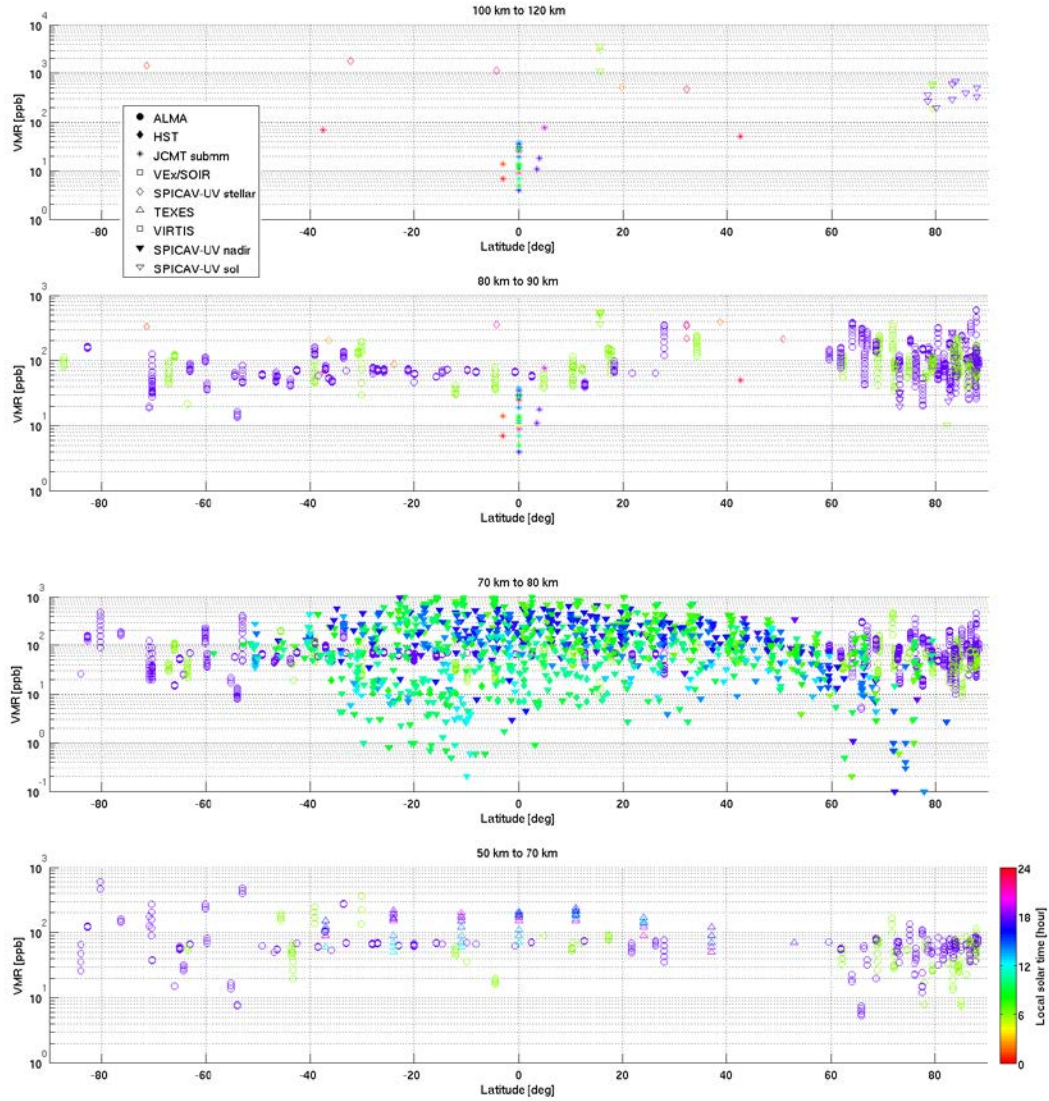


Figure 8:  $\text{SO}_2$  VMR values as a function of latitude for different altitude regions, from top to bottom: 100 to 120 km (Panel top left), 80 to 90 km (Panel top right), 70 to 80 km (Panel bottom left) and 50 to 70 km (Panel bottom right). The colour code is the local solar time and the symbols are the instruments.

The dominant trend inferred from the SPICAV-UV nadir observations presented in Figure 8 is that  $\text{SO}_2$  levels on the dayside (mid-AM to mid-afternoon) are maximum near 15S latitude and then decrease towards the poles. Though it is difficult to discern from Figure 8, the opposite latitudinal gradient was also sometimes evident in the SPICAV-UV nadir data [12]. Similarly, the 2010 and 2011 HST observations showed that the cloud top  $\text{SO}_2$  abundance latitudinal distribution was centred at  $\pm 15^\circ$  latitude, and that the gradient in latitude changed from date to date depending on the magnitude of the  $\text{SO}_2$  abundance observed at the equator.

The timing and observed variation of the cloud top  $\text{SO}_2$  abundance derived from the 2010 and 2011 HST observations confirmed that it is highly variable on week to month-long time scales, as would be expected based on previous Pioneer Venus observations and the full

SPICAV nadir dataset. The January 2011 HST observations specifically showed that within 4.9 Earth days (which is comparable to Venus'  $4.6 \pm 0.3$  Earth-day cloud-top rotation time scale) (i) the low-latitude  $\text{SO}_2$  density dropped; (ii) the latitudinal gradient of the  $\text{SO}_2$  gas between 10N and 35S reversed from increasing with decreasing latitude; and (iii) the  $0.24 \mu\text{m}$  cloud brightness level (which is indicative of the overall sub-micron haze density) also declined. Moreover, the  $0.365 \mu\text{m}$  VMC observations obtained in the same period showed that between the two January 2011 HST observation dates, changes in the cloud top brightness levels were only observed north of 35S latitude, thus overlapping the region where a significant change in the  $\text{SO}_2$  latitudinal gradient occurred. This provides further evidence that Venus'  $0.36 \mu\text{m}$  cloud brightness, submicron haze density and  $\text{SO}_2$  gas abundance are all inter-related [30].

The time scale on which the decline in both the  $\text{SO}_2$  abundance and the  $0.24 \mu\text{m}$  cloud brightness level were observed and the coincident reversal in the  $\text{SO}_2$  latitudinal gradient corroborated the trends inferred from SPICAV-UV nadir observations. In particular, Marcq et al. [12] hypothesized that variations in  $\text{SO}_2$  density are related to changes in convective mixing in the upper cloud at low latitudes. They further hypothesized that a decrease in the upward pumping of both the  $\text{SO}_2$  gas and other collocated aerosols near the equator combined with the on-going efficient photolysis of the gas at low-latitudes, produces a slow decline in the equatorial gas density while the change in the downward flux and photochemical processing of the gas and aerosols at higher latitudes (and high solar zenith angles) is limited. Thus, the impact of supply fluctuations on  $\text{SO}_2$  abundances is most prominent at low-latitudes. Additionally, if the convective mixing is sufficiently low, the factors described above will reverse the latitudinal gradient of the gas density within 5 days, from increasing with decreasing latitude to decreasing with decreasing latitude.

#### 3.1.4 Interpretation of short-term and short-scale variability

The motion of the  $\text{SO}_2$  maximum observed from one day to the next in the upper cloud deck near 60 km (see Figure 3) cannot be explained by winds, since they would imply meridional winds much higher than observed [31]. Since the photochemical modelling presented in [14] indicates that zonal and vertical transport dominates over  $\text{SO}_2$  photolysis between 60 and 70 km at all solar zenith angles, the high  $\text{SO}_2$  variability cannot be explained solely by its photolysis. Therefore, if the observed variability is chemically driven, it must involve additional reactions that impact the sulfur and/or oxygen budget at those altitudes.

The  $\text{SO}_2$  abundance below the clouds is about 1000 times higher than above. It is conceivable that the strong spatial and temporal variability of  $\text{SO}_2$  on short scales is related to localized perturbations to the vertical mixing rate of  $\text{SO}_2$ . For example, localized enhancements of sulfur dioxide could rise to the cloud top level via small convective cells and could disappear over a short time scale due to photodissociation or formation of  $\text{SO}_3$  [11, 12, 23]. This mechanism is consistent with the simple model of  $\text{SO}_2$  latitudinal variability first presented in Marcq et al. [12] and discussed above, which requires a photochemical sink for  $\text{SO}_2$  acting in about  $10^4$  to  $10^5$  s (ranging from a few hours to about one Earth day) in order to explain the

opposite latitudinal patterns during SO<sub>2</sub>-rich and SO<sub>2</sub>-poor epochs [12, 14]. However, a unique physical mechanism has yet to be identified that can explain how the SO<sub>2</sub> gas is transported through the dynamically stable atmospheric layer known to be located in the region between Venus' lower and upper atmosphere.

Above 80 km the modelled SO<sub>2</sub> photodissociation rate is faster than the zonal and vertical transport rates and observations have indicated that at least one additional significant sulfur reservoir (besides SO<sub>2</sub> and SO) must be present. This additional sulfur reservoir has been tentatively attributed to sulfur-bearing aerosols [32, 33], but their exact nature is still not known. Consequently, it is likely that observed localised temporal variations of sulfur species at 80-100 km are driven by photochemistry, condensation/evaporation, and/or small-scale atmospheric perturbations such as gravity waves. Note that the variability of water at these altitudes is thought to result from short-scale and short-term variations of the temperature in the upper mesosphere [34]. Larger scale variations of sulfur species in the upper mesosphere might be the result of changes in the high-altitude circulation.

### **3.2 Long-term variations**

Based on the data considered in this study, which cover the time period from 2004 to 2014, the long-term (i.e. > atmospheric rotation rate) variability of SO<sub>2</sub> in the atmosphere of Venus can be investigated. Figure 9 illustrates the long-term evolution of the SO<sub>2</sub> abundance with time for different altitude ranges, the instruments being represented by different symbols and the colour showing the latitude at which the measurements were performed. At low latitudes (blue/cyan/lime symbols in the figure) higher SO<sub>2</sub> abundances are observed above 70 km between 2007 and 2008 followed by a decrease the following years. The long-term variations of SO<sub>2</sub> seen in the 70-80 km region at low latitudes by SPICAV-UV nadir observations [12] were already mentioned in the introduction. To summarize, the SO<sub>2</sub> column density observed in mid to late 2007 was factor of 2 higher than first observed in 2006, while subsequent to this time the abundance decreased slowly (superimposed with a much larger short-term variability) by a factor of 5-10 between 2008 and late 2012. This asymmetry between a relatively smooth and rapid increase on one hand, and a much slower and more irregular decrease on the other hand was also observed by PVO [6] thirty years earlier, suggesting that it is representative of the behaviour of SO<sub>2</sub> on a decennial time scale. Assuming, as discussed above, that the observed low-latitude SO<sub>2</sub> abundance is strongly dependent on the supply of SO<sub>2</sub> from lower altitudes, then the observed pattern may be a direct indicator of a significant injection of SO<sub>2</sub> at low latitudes on a decennial time scale.

Even though in each panel the low-latitude occultation data reveal a trend wherein the SO<sub>2</sub> abundance between 2007 and 2008 is higher than observed at other times in all altitude ranges, there is not any occultation data in the 100-120 km range beyond 2009. So, in the 100-120 km panel the apparent “decreases” in the SO<sub>2</sub> abundance beyond the 2007-2008 time period are primarily substantiated by the fact that JCMT data are compared to the occultation data. But we cannot use the comparison of these two datasets to determine temporal variability in this altitude range since the JCMT does not show increase in SO<sub>2</sub> abundance as

a function of altitude, i.e., since the JCMT and occultation retrievals overlap in the 80-90 km region. It follows that the JCMT data will always be inherently lower than the occultation retrievals wherein the  $\text{SO}_2$  abundance increases with altitude.

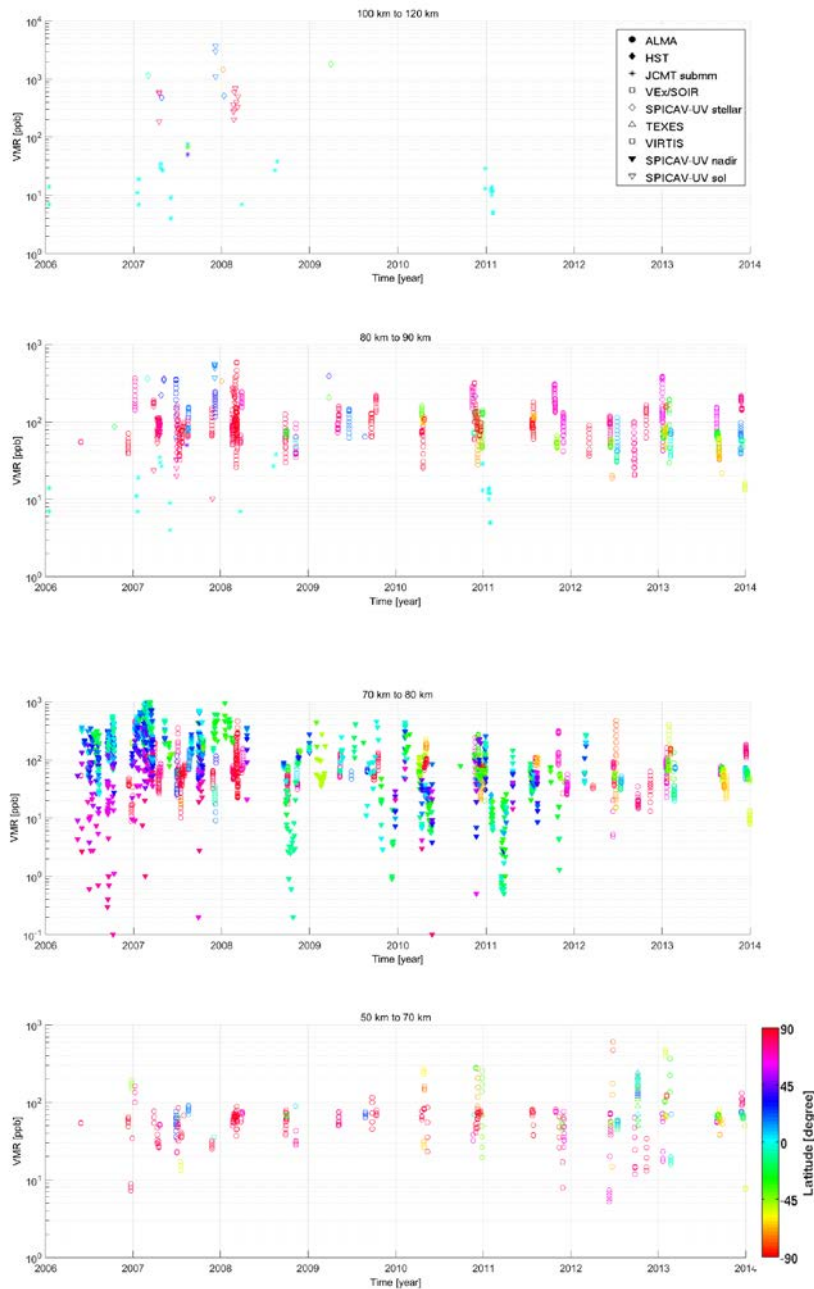


Figure 9:  $\text{SO}_2$  VMR values as a function of time for different altitude regions, from top to bottom: 100 to 120 km, 80 to 90 km, 70 to 80 km and 50 to 70 km. The colour code is the latitude and the symbols represent the instruments.

Variability of  $\text{SO}_2$  on time scales shorter than one Venusian year (224.7 Earth days), but longer than the super-rotation period (4 to 5 Earth days at the UV cloud top) can be studied thanks to the extensive SPICAV-UV data set, using the Lomb-Scargle algorithm [35, 36]. This method is especially suited to irregularly sampled data such as SPICAV-UV nadir observations. A drawback of this algorithm is that “ghost” harmonics may appear for integer multiples of the fundamental modes. The result is shown on Figure 10. The 1-(24 hour) day, and likely the 224.7-(24 hr) day, periods are artefacts caused by the VEx 24 hour orbital period affecting the sampling of SPICAV-UV observations. But the 117-(24 hour) day period, equal to the Venusian solar day at the solid surface, suggests a coupling between the zonal circulation and the  $\text{SO}_2$  abundance, since this 117-day period was also detected by VMC cloud tracking of the zonal wind speed at the UV cloud top [37]. Moreover, this 117-day period also suggests a coupling between the surface and the general circulation at the UV cloud top level, perhaps through gravity waves forced by the topography that could propagate upwards and break in the cloud region, affecting both zonal wind speeds (through zonal momentum deposition) and  $\text{SO}_2$  through enhanced associated convective mixing [38].

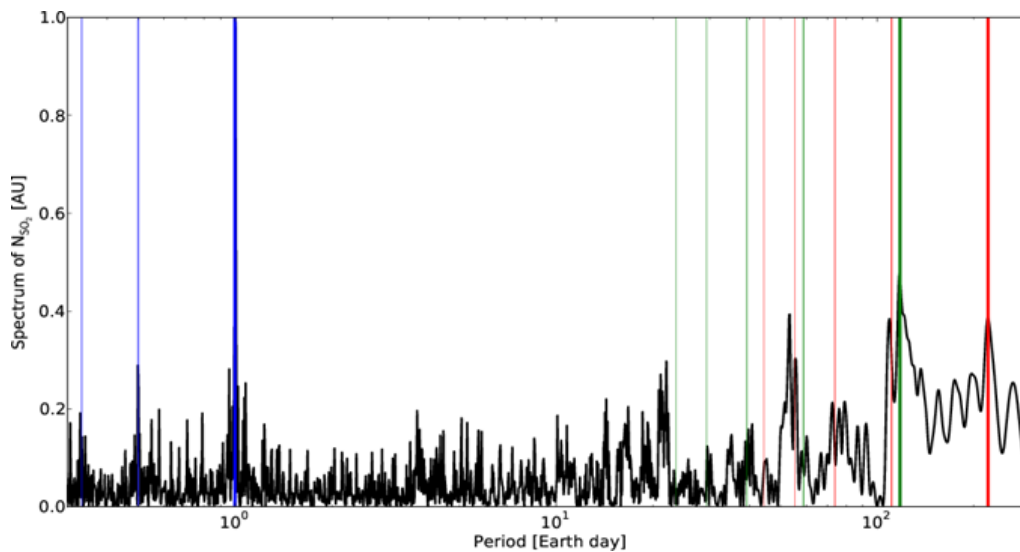


Figure 10: Lomb-Scargle periodogram of SPICAV-UV nadir  $\text{SO}_2$  column densities at low latitudes. The blue, green and red lines are located at periods of 1day, 117 days and 224.7days respectively.

## 4 Recommendations and conclusions

### 4.1 Laboratory support

Laboratory work underpins the observations and modelling summarised here and updates to laboratory data can have significant effects on the interpretation of both observations and modelling. One example is the changes shown in Part I of this series in the modelled

behaviour of SO<sub>2</sub> near the cloud-top when using temperature-dependent SO<sub>2</sub> cross sections [39-47].

Some recent studies (e.g., [33, 48-50]) have identified laboratory work that is critical for further quantitative advances in understanding SO<sub>2</sub> on Venus. Amongst the most critical laboratory studies that are required to improve modelling efforts are measurements of rate coefficients for reactions producing and destroying ClSO<sub>2</sub>, ClSO<sub>4</sub>, and SO<sub>2</sub>Cl<sub>2</sub>. The limited rate coefficient data presently available for reactions producing and destroying these species should be verified. Rate coefficients for other potentially important reactions also need to be experimentally determined for the first time. UV cross sections and photo-dissociation branching ratios for ClSO<sub>2</sub>, ClSO<sub>4</sub>, and SO<sub>2</sub>Cl<sub>2</sub>, as well as for S<sub>2</sub>O and (SO)<sub>2</sub>, are required for photochemical modelling and to assess their potential as candidates for the unidentified UV absorber. Previous attempts to obtain spectra of S<sub>2</sub>O and (SO)<sub>2</sub> failed to uniquely identify which sulfur-bearing compounds were present [51], thus the currently published spectra need confirmation. Recent ab initio work [2] has taken a major step towards addressing these gaps but requires experimental confirmation. Cross sections, comparable in quality to the high-resolution, temperature-dependent ones measured for SO<sub>2</sub>, are required for SO in the UV and for H<sub>2</sub>SO<sub>4</sub> in the UV-visible. This latter work is also needed to support observational studies. Additional laboratory work needed in support of observational studies includes the acquisition of S-band HSO<sub>3</sub> and SO<sub>3</sub> spectra for interpreting radio occultation data from *Venus Express* and identification and measurement of submillimetre SO<sub>3</sub> bands that can be observed from ground-based telescopes. Finally, SOFIA flies at a sufficiently high altitude so that new, previously unobservable, bands for SO, SO<sub>2</sub>, SO<sub>3</sub>, HSO<sub>3</sub>, H<sub>2</sub>SO<sub>4</sub>, H<sub>2</sub>O, and HDO may be accessed [24, 52]. These bands may offer improved sensitivity for some species and/or they may probe different altitude regions in Venus' atmosphere than bands that are accessible from the Earth's surface. But, SO<sub>x</sub> spectra at the range of wavelengths observable from SOFIA are needed to make efficient use of its capabilities.

Many unknowns continue to limit understanding of the cloud layers on Venus, particularly the connections between gas- and condensed-phase sulfur species. Verification of the rate coefficient and mechanism for production of H<sub>2</sub>SO<sub>4</sub> from H<sub>2</sub>O and SO<sub>3</sub>, as well as alternate paths for production of H<sub>2</sub>SO<sub>4</sub>, viable for the conditions present in Venus' atmosphere are still needed. Likewise, the rate coefficient for association of SO<sub>2</sub> and O to form SO<sub>3</sub> under Venus' conditions is required. Further laboratory work on the physical chemistry of sulfuric acid at 150-300 K is needed to determine equilibrium vapour pressures for H<sub>2</sub>SO<sub>4</sub>, H<sub>2</sub>O, SO<sub>3</sub>, and SO<sub>2</sub> over 70-95 wt% sulfuric acid because extrapolations of existing thermodynamic models to these conditions produce significantly different results [33, 51].

#### **4.2 Conclusions and perspectives**

Observations of Venus' SO<sub>2</sub> distribution obtained using VEx and Earth-based observatories during the 9-year VEx mission indicate that Venus' SO<sub>2</sub> gas distribution varies rapidly on short time scales throughout the 60-100 km altitude region [14, 23, 29, 53, 54]. Averaging the

short-time scale variations observed by VEx/SPICAV at low-latitude on Venus over a full Earth year, for each year of the VEx, mission indicates that the SO<sub>2</sub> gas abundances in the upper cloud deck were high ( $\geq 400$  ppb) in 2007 [11, 19]. However, for the remainder of the mission a consistent decline in the SO<sub>2</sub> gas abundance was observed [12]. Upper cloud SO<sub>2</sub> abundance record indicates that dramatic increases in the 70-80 km SO<sub>2</sub> abundance may be episodic in nature [12], and if so, the driver of this behaviour cannot be explained as a function of local time variations but may be an indication of the existence of episodic events, such as a volcanic eruption, an episodic large dynamical instability within the atmosphere, a large scale change in the general circulation. The decline of SO<sub>2</sub> subsequent to a sharp increase is slow: only 30% decrease within one year after the inflation event.

The large day-to-day variability seen in mesospheric SO<sub>2</sub> at several different altitudes between 60 and 100 km, are not yet explained. Maps of the horizontal spatial extent of SO<sub>2</sub> enhancements, as revealed by TEXES observations, have proven particularly instructive in revealing the morphology and timescale. Patterns in the overall SO<sub>2</sub> abundance and the observed SO<sub>2</sub> latitudinal gradient over the lifetime of both the HST and SPICAV nadir observations suggest that both are dependent on fluctuations in the supply of the SO<sub>2</sub> gas from lower altitudes. However, the exact mechanisms that support the cloud-level chemistry and transport through the cloud layer are still unknown.

Full disk mapping of the local time behaviour throughout the 40-100 km region are highly valuable for understanding how the upper and lower cloud regions are linked, both chemically and dynamically, particularly in the near terminator region, where the transition from day to night impacts temperature, zonal winds, convection, and photolysis rates.

In order to resolve the issues that relate to Venus' sulfur-cycle and H<sub>2</sub>SO<sub>4</sub> formation, additional observations that can explore and characterize Venus' chemical, dynamical and microphysical processes over a wide range of altitudes are needed on a consistent basis. This will require in situ investigations in the clouds of Venus from probes and/or aerial platforms, in conjunction with simultaneous remote sounding. The best way to explore and investigate the science questions that remain unresolved subsequent to the Venus Express era is probably through combined Earth-based and Venus orbiting observations. Even with the successful insertion of Japan's *Akatsuki* mission, unless additional Venus missions are selected in the near future, the burden to maintain regular measurement of the SO<sub>2</sub> abundance and distribution in the time period beyond 2019 will be dependent entirely on Earth-based observing opportunities. In this case, an on-going Earth-based observing program is critical to retaining a usable record of both the long-term and short-term variability within Venus' atmosphere, so that the physical processes that control the sulfur-oxide cycle on Venus can be fully interpreted. For example, to further study the nature of the spatial and temporal variations, observations that characterize the SO<sub>2</sub> variability at multiple altitudes without any temporal or spatial confusion or disparity are needed. For this reason, simultaneous sampling of the gas abundance at different altitudes would provide unprecedented insight into the impact of vertical mixing, photochemistry, aerosol microphysics, and meridional transport on

Venus' SO<sub>2</sub> gas inventory. These data can be obtained at multiple wavelengths (thereby sensing multiple altitudes), using both remote and in-situ observing platforms. Joint HST (200-300 nm, z ~ 65-80 km sensitivity), ALMA (sub-mm, z > 70 km) and TEXES (mid-IR, z ~ 60-70 km) data could allow for the investigation of local time and latitudinal SO<sub>2</sub> gas abundance variation in three key altitude regimes, while also simultaneously measuring the SO variability at altitudes greater than 70 km, as well as the H<sub>2</sub>O density above and below the 70-80 km region. Such coordinated observations should be carried out on a daily basis over the time scale of Venus' cloud rotation cycle. Moreover, repeated and regular coordinated observations on the time scale of the cloud rotation cycle would allow us to begin to understand the sources of the short and long term variability within the mesosphere.

## Acknowledgements

The authors wish to thank the International Space Science Institute (ISSI) for their fruitful support. Most of the authors were members of the ISSI International Team "Sulfur Dioxide variability in the Venus atmosphere" which met during 2013-2015 in the facilities of ISSI in Bern, Switzerland.

*Venus Express* is a mission of the European Space Agency. The James Clerk Maxwell Telescope is operated by the Joint Astronomy Centre on behalf of the Science and Technology Facilities Council of the United Kingdom, the National Research Council of Canada, and (until 31 March 2013) the Netherlands Organisation for Scientific Research. Investigator Sandor was supported by the U.S. National Science Foundation under Grant no. AST-1312985, and by NASA under Grant nos NNX10AB33G, NNX12AI32G and NNX14AK05G. F.P. Mills also acknowledges partial support under NASA Grant NNX12AI32G to Space Science Institute. The research program was supported in Belgium by the Belgian Federal Science Policy Office and the European Space Agency (ESA, PRODEX program, contracts C 90268, 90113, and 17645). Some authors also recognize the support from the FP7 EuroVenus project (G.A. 606798). We acknowledge the support of the "Interuniversity Attraction Poles" program financed by the Belgian government (Planet TOPERS). This research was also supported by a BRAIN research grant BR/143/A2/SCOOP of the Belgian Federal Science Policy Office. A. Mahieux thanks the FNRS for the position of "*chargé de recherche*". O. Korablev, D. Belyaev acknowledge support from Roscosmos and the Russian Academy of Science (FANO). E. Marcq, F. Montmessin, F. Lefèvre and A. Stolzenbach acknowledge support from CNES and from the Programme National de Planétologie (PNP) of CNRS/INSU. Co-authors affiliated at IKI and LATMOS/CNRS acknowledge support from the FRRI #10-52-16011 in frames of Russian-French GDRI cooperation. C. D. Parkinson also acknowledges support with funding in part by NASA Grant #NNX11AD81G to the University of Michigan. The HST observations were obtained through NASA/HST program 12433. Support for this program was provided through a grant from

Space Science Telescope Institute, which is operated by the Association of Universities for Research in Astronomy, Inc., under NAS5-26555. Additional funding for the analysis of the HST observations was provided through funding from the NASA Early Careers Program, NASA Grant NNX11AN81G and the NASA Planetary Atmospheres Program, Grant NNX12AG55G. The authors would additionally like to acknowledge Adriana Ocampo, NASA Headquarters, John Grunsfield, NASA Headquarters, Alan Stern, SwRI, Claus Leither, Space Telescope Science Institute, and Håkan Svedhem, *Venus Express* Project Scientist for their support in the acquisition of the joint HST-*Venus Express* Venus Observing Campaign.

## References

1. Esposito, L.W., *Ultraviolet contrasts and the absorbers near the Venus cloud tops*. J. Geophys. Res. 1980. **85**: p. 8151-8157.
2. Frandsen, B.N., P. Wennberg, and H.G. Kjaergaard, *Identification of OSSO as a near-UV absorber in the Venusian atmosphere*. Geophys. Res. Lett., 2016. **43**(21): p. 11146-11155.
3. Lee, Y.L., et al., *Long-term variations of the UV contrast on Venus observed by the Venus Monitoring Camera on board Venus Express*. Icarus, 2015. **253**: p. 1-15.
4. Sandor, B., R.T. Clancy, and G. Moriarty-Schieven, *Upper limits for H<sub>2</sub>SO<sub>4</sub> in the mesosphere of Venus*. Icarus, 2012. **217**(2): p. 839-844.
5. Stewart, A.I., et al., *Ultraviolet Spectroscopy of Venus: Initial Results from the Pioneer Venus Orbiter*. Science, 1979. **203**: p. 777-779.
6. Esposito, L.W., et al., *Sulfur Dioxide at the Venus Cloud Tops, 1978–1986*. J. Geophys. Res., 1988. **93**(D5): p. 5267–5276.
7. Na, C.Y., L.W. Esposito, and T.E. Skinner, *International Ultraviolet Explorer Observation of Venus SO<sub>2</sub> and SO*. J. Geophys. Res., 1990. **95**(D6): p. 7485–7491.
8. McClintock, W.E., C.A. Barth, and R.A. Kohnert, *Sulfur Dioxide in the Atmosphere of Venus: I. Sounding Rocket Observations*. Icarus, 1994. **112**(2): p. 382-388.
9. Na, C.Y., et al., *Sulfur Dioxide in the Atmosphere of Venus: II. Modeling Results*. Icarus, 1994. **112**(2): p. 389-395.
10. Na, C.Y. and L. Esposito. *UV Observation of Venus with HST*. in *27th AAS/DPS Annual Meeting, Hawaii, Oct. 9-13. 1995*.
11. Marcq, E., et al., *An investigation of the SO<sub>2</sub> content of the venusian mesosphere using SPICAV-UV in nadir mode*. Icarus, 2011. **211**: p. 58–69.
12. Marcq, E., et al., *Variations of sulphur dioxide at the cloud top of Venus's dynamic atmosphere*. Nature Geoscience, 2013. **6**: p. 25-28.
13. Esposito, L.W., et al., *Chemistry of lower atmosphere and clouds*, in *Venus II: Geology, Geophysics, Atmosphere, and Solar Wind Environment*, S.W. Bougher, D.M. Hunten, and R.J. Phillips, Editors. 1997, Univ. of Arizona Press. p. 415-458.
14. Jessup, K.L., et al., *Coordinated Hubble Space Telescope and Venus Express Observations of Venus' upper cloud deck*. Icarus, 2015. **258**: p. 309–336.
15. Bertaux, J.L., et al., *SPICAM on Mars Express: Observing modes and overview of UV spectrometer data and scientific results*. J. Geophys. Res., 2006. **111**(E10S90).
16. Bertaux, J.L., et al., *SPICAV on Venus Express: Three spectrometers to study the global structure and composition of the Venus atmosphere*. Planet. Space Sci., 2007. **55**(12): p. 1673-1700.
17. Thuillier, G., et al., *SOLAR/SOLSPEC: Scientific Objectives, Instrument Performance and Its Absolute Calibration Using a Blackbody as Primary Standard Source*. Solar Physics, 2009. **257**: p. 185-213.
18. Belyaev, D., et al., *First observations of SO<sub>2</sub> above Venus' clouds by means of solar occultation in the infrared*. J. Geophys. Res., 2008. **113**: p. doi:10.1029/2008JE003143.
19. Belyaev, D., et al., *Vertical profiling of SO<sub>2</sub> and SO above Venus' clouds by SPICAV/SOIR solar occultations*. Icarus, 2012. **217**(2): p. 740-751.
20. Lacy, J., PASP, 2002. **111**: p. 153.
21. Encrenaz, T., et al., *Hydrogen peroxide on Mars: evidence for spatial and seasonal variations*. Icarus, 2004. **170**(2): p. 424-429.
22. Encrenaz, T., et al., *Hydrogen peroxide on Mars: Observations, interpretation and future plans*. Planet. Space Sci., 2012. **68**: p. 3-17.

23. Encrenaz, P., et al., *HDO and SO<sub>2</sub> thermal mapping on Venus: evidence for strong SO<sub>2</sub> variability*. *Astron. Astrophys.*, 2012. **543**: p. 10.1051/0004-6361/201219419.
24. Encrenaz, T., et al., *HDO and SO<sub>2</sub> thermal mapping on Venus. II. The SO<sub>2</sub> spatial distribution above and within the clouds*. *Astron. Astrophys.*, 2013. **559**(A65): p. DOI: 10.1051/0004-6361/201322264.
25. Encrenaz, T., et al. *HDO and SO<sub>2</sub> thermal mapping on Venus above and within the clouds*. in *EPSC Conference*. 2014. Cascais, Portugal, 7-12 September
26. Encrenaz, T., et al., *HDO and SO<sub>2</sub> thermal mapping on Venus*. *Astron. Astrophys.*, 2016. **595**: p. A74.
27. Encrenaz, T., et al., *Submillimeter mapping of mesospheric minor species on Venus with ALMA*. *Planet. Space Sci.*, 2015. **113**: p. 275-291.
28. Ignatiev, N.I., et al., *Altimetry of the Venus cloud tops from the Venus Express observations*. *J. Geophys. Res.*, 2009. **114**: p. doi:10.1029/2008JE003320.
29. Sandor, B.J., et al., *Sulfur Chemistry in the Venus Mesosphere from SO<sub>2</sub> and SO Microwave Spectra*. *Icarus*, 2010. **208**(1): p. 49-60.
30. Titov, D., et al., *Morphology of the cloud tops as observed by the Venus Express Monitoring Camera*. *Icarus*, 2012. **217**(2): p. 682-701.
31. Hueso, R., J. Peralta, and A. Sanchez-Lavega, *Assessing the long-term variability of Venus winds at cloud level from VIRTIS–Venus Express*. *Icarus*, 2012. **217**(2): p. 585-598.
32. Zhang, X., et al., *Photolysis of sulphuric acid as the source of sulphur oxides in the mesosphere of Venus*. *Nature Geoscience*, 2010. **3**: p. 834-7.
33. Zhang, X., et al., *Sulfur chemistry in the middle atmosphere of Venus*. *Icarus*, 2012. **217**(2): p. 714-739.
34. Gurwell, M.A., et al., *SWAS observations of water vapor in the Venus mesosphere*. *Icarus*, 2007. **188**(2): p. 288-304.
35. Lomb, N.R., *Least-squares frequency analysis of unequally spaced data*. *Astrophysics and Space Science*, 1976. **39**: p. 447-462.
36. Scargle, J.D., *Studies in astronomical time series analysis. II - Statistical aspects of spectral analysis of unevenly spaced data*. *Astrophys. J.*, 1982. **263**: p. 835-853.
37. Khatuntsev, I., et al., *Cloud level winds from the Venus Express Monitoring Camera imaging*. *Icarus*, 2013. **226**(1): p. 140-158.
38. Bertaux, J.L., et al., *Observed influence of Venus topography on the zonal wind and albedo at cloud top level*. *J. Geophys. Res.* 2016 (acc. for publication).
39. Blackie, D., et al., *High-resolution photoabsorption cross-section measurements of SO<sub>2</sub> at 198 K from 213 to 325 nm*. *J. Geophys. Res.* 2011. **116**(E03006): p. doi: 10.1029/2010JE003707.
40. Blackie, D., et al., *Correction to High-resolution photoabsorption cross-section measurements of SO<sub>2</sub> at 198 K from 213 to 325 nm*. *J. Geophys. Res.* 2011. **116**(E12099): p. doi: 10.1029/2011JE003977.
41. Bogumil, K., et al., *Measurements of molecular absorption spectra with the SCIAMACHY pre-flight model: Instrument characterization and reference data for atmospheric remote-sensing in the 230-2380 nm region*. *J. Photochem. Photobiol., A: Chemistry*, 2003. **157**(2-3): p. 167-184.
42. Feng, R., et al., *Absolute photoabsorption oscillator strengths by electron energy loss methods: the valence and S 2p and 2s inner shells of sulphur dioxide in the discrete and continuum regions (3.5-260 eV)*. *Chem. Phys.*, 1999. **240**: p. 371-386.
43. Golomb, D., K. Watanabe, and F.F. Marmo, *Absorption Coefficients of Sulfur Dioxide in the Vacuum Ultraviolet*. *J. Chem. Phys.*, 1962. **36**(4): p. 958-960.

44. Rufus, J., et al., *High-resolution photoabsorption cross-section measurements of SO<sub>2</sub> at 160 K between 199 and 220 nm*. J. Geophys. Res., 2009. **114**(E06003).
45. Vandaele, A.C., C. Hermans, and S. Fally, *Fourier Transform measurements of SO<sub>2</sub> absorption cross sections: II. Temperature dependence in the 29 000 - 44 000 cm<sup>-1</sup> (227-345 nm) region*. J. Quant. Spectrosc. Radiat. Transfer, 2009. **110**: p. 2115-2126.
46. Warneck, P., F.F. Marmo, and J.O. Sullivan, *Ultraviolet absorption of SO<sub>2</sub>: Dissociation energies of SO<sub>2</sub> and SO*. J. Chem. Phys., 1964. **40**(4): p. 1132-1136.
47. Wu, R.C.Y., et al., *Measurements of High-, Room-, and Low-Temperature Photoabsorption Cross Sections of SO<sub>2</sub> in the 2080- to 2950-A° Region, with Application to Io*. Icarus, 2000. **145**: p. 289-296.
48. Krasnopolsky, V.A., *A photochemical Model for the Venus Atmosphere at 47-112 km*. Icarus, 2012. **218**(1): p. 230-246.
49. Mills, F.P. and M. Allen, *A review of selected issues concerning the chemistry in Venus' middle atmosphere*. Planet. Space Sci., 2007. **55**(12): p. 1729-1740.
50. Mills, F.P., L.W. Esposito, and Y.L. Yung, *Atmospheric composition, chemistry and clouds*. Geophysical Monograph Series, 2007. **176**: p. 73-100.
51. Mills, F., *I. Observations and photochemical modeling of the Venus middle atmosphere. II. Thermal infrared spectroscopy of Europa and Callisto*. 1998, California Institute of Technology.
52. Cuzzi, J., et al., *Planetary Science*, in *The Science Vision for the Stratospheric Observatory for Infrared Astronomy*, R. Gehrz, Editor. 2009, NASA Technical Report, NASA Ames Research Center, Moffett Field, California, USA.
53. Jessup, K.L., et al. *HST/STIS Observations of Venus' Dayside Atmosphere, from morning to noon*. in *46th DPS, BAAS, #302.01*. 2014.
54. Marcq, E., et al., *Search for horizontal and vertical variations of CO in the day and night side lower mesosphere of Venus from CSHELL/IRTF 4.53 μm observations*. Planet. Space Sci., 2015. **113-114**: p. 256-263.